Published in final edited form as:
J Immunol. 2005 August 15; 175(4): 2563–2569.

Immune Regulation of Protease-Activated Receptor-1 Expression in Murine Small Intestine during *Nippostrongylus brasiliensis* Infection

Aiping Zhao[*,†], **Motoko Morimoto**[*,†], **Harry Dawson**[†], **Justin E. Elfrey**[*], **Kathleen B. Madden**[‡], **William C. Gause**[§], **Booki Min**[¶], **Fred D. Finkelman**[‖], **Joseph F. Urban Jr**[†], and **Terez Shea-Donohue**[2,*,†]

*****Department of Medicine and the Mucosal Biology Research Center, University of Maryland School of Medicine, Baltimore, MD 21201

†Nutritional Requirements and Functions Laboratory, Beltsville Human Nutrition Research Center, Agricultural Research Service, U.S. Department of Agriculture, Beltsville, MD 20705

‡Department of Pediatrics, Uniformed Services University of the Health Sciences, Bethesda, MD 20814

§Department of Microbiology and Immunology, Uniformed Services University of the Health Sciences, Bethesda, MD 20814

¶Laboratory of Immunology, National Institute of Allergy and Infectious Diseases, National Institutes of Health, Bethesda, MD 20892

Departments of Medicine and Pediatrics, University of Cincinnati, Cincinnati, OH 45267 and Cincinnati Veterans Administration Medical Center, Cincinnati, OH 45220

Abstract

Infection with gastrointestinal nematodes exerts profound effects on both immune and physiological responses of the host. Helminth infection induces a hypercontractility of intestinal smooth muscle that is dependent on the Th2 cytokines, IL-4 and IL-13, and may contribute to worm expulsion. Protease-activated receptors (PARs) are expressed throughout the gut, and activation of PAR-1 was observed in asthma, a Th2-driven pathology. In the current study we investigated the physiologic and immunologic regulation of PAR-1 in the murine small intestine, specifically 1) the effect of PAR-1 agonists on small intestinal smooth muscle contractility, 2) the effects of *Nippostrongylus brasiliensis* infection on PAR-1 responses, 3) the roles of IL-13 and IL-4 in *N. brasiliensis* infection-induced alterations in PAR-1 responses, and 4) the STAT6 dependence of these responses. We demonstrate that PAR-1 activation induces contraction of murine intestinal smooth muscle that is enhanced during helminth infection. This hypercontractility is associated with an elevated expression of PAR-1 mRNA and protein. *N. brasiliensis*-induced changes in PAR-1 function and expression were seen in IL-4-deficient mice, but not in IL-13- or STAT6-deficient mice, indicating the dependence of IL-13 on the STAT6 signaling pathway independent of IL-4.

Protease-activated receptors (PARs) are a novel subclass of seven transmembrane-spanning, G protein-coupled receptors that contain their own ligand. PARs are activated by a unique mechanism that involves recognition of the receptor by a protease, cleavage of the receptor at a specific enzymatic site located at the extracellular NH_2 terminus, and finally, exposure of a

2 Address correspondence and reprint requests to Dr. Terez Shea-Donohue, Mucosal Biology Research Center, University of Maryland School of Medicine, 20 Penn Street, Baltimore, MD 21201. E-mail address: tdonohue@mbrc.umaryl.edu

Disclosures
The authors have no financial conflict of interest.

new N-terminal domain that acts as a tethered ligand, binding and activating the receptor itself (1,2). Four PAR family members have been identified to date: PAR-1, PAR-3, and PAR-4, which are activated specifically by thrombin, and PAR-2, which is activated by trypsin or human mast cell tryptase. PARs are expressed in a variety of tissues, including the gastrointestinal tract (1,3).

PAR-1, the first PAR to be cloned (4), is involved in a variety of physiological and pathophysiological activities, including platelet aggregation, vascular and airway smooth muscle relaxation/contraction, nerve regeneration, and immune responses (1,5). PAR-1 is expressed throughout the gut, where it has been identified in smooth muscle, epithelial, nerve, and lamina propria cells. Gut PAR-1 expression appears to have important physiological consequences, because PAR-1 activation stimulates intestinal epithelial cell secretion (6,7); induces smooth muscle relaxation and contraction of the stomach, small intestine, and colon (with contraction predominating) (8–10); and promotes in vivo gastrointestinal transit (11).

PAR-1 activation was observed in inflammatory disorders that are associated with Th2 cytokines, including asthma (2). The same Th2 cytokines that are associated with asthma pathogenesis, particularly IL-4 and IL-13, are also up-regulated in the small intestine during intestinal helminth infections, where they induce stereotypic changes in epithelial and smooth muscle function that facilitate worm expulsion (12,13). Induction of these stereotypic changes by both IL-4 and IL-13 requires cytokine binding to the type 2 IL-4R (IL-4Rα/IL-13Rα1) and subsequent IL-4R activation of the transcription factor STAT6 (14). Because both IL-4/IL-13 and PAR-1 have been implicated in changes in intestinal physiology that may promote worm expulsion from the gut and have been associated with the pathogenesis of asthma, we hypothesized that PAR-1 might be involved in the physiological effects of IL-4 and IL-13. To investigate this possibility, we have evaluated 1) the effect of PAR-1 agonists on small intestinal smooth muscle contractility, 2) the effects of *Nippostrongylus brasiliensis* infection on PAR-1 responses, 3) the roles of IL-13 and IL-4 in *N. brasiliensis* infection-induced alterations in PAR-1 responses, and 4) the STAT6 dependence of these responses. The results of these investigations demonstrate that PAR-1 activation induces contraction of intestinal smooth muscle that is enhanced during helminth infection. This hypercontractility is associated with an elevated expression of PAR-1 mRNA and protein, and these helminth-induced changes in PAR-1 function and expression are dependent on the IL-13-activated STAT6 signaling pathway independently of IL-4.

Materials and Methods

Mice

BALB/c female mice (wild type (WT)) were purchased from the Small Animal Division of the National Cancer Institute. BALB/c STAT6-deficient mice (STAT6$^{-/-}$), IL-4-deficient mice (IL-4$^{-/-}$), and IL-13-deficient mice (IL-13$^{-/-}$) mice were obtained from the breeding colonies at the Uniformed Services University of the Health Sciences and National Institutes of Health, respectively. These studies were conducted in accordance with principles set forth in the Guide for Care and Use of Laboratory Animals, Institute of Laboratory Animal Resources, National Research Council, Health and Human Services and the Beltsville Animal Care and Use Committee, 2003.

Administration of IL-13

Mice (n = 7/group) were injected i.v. with 10 μg of saline or IL-13 daily for 7 days. The amount of cytokine administered was based on the observation that daily injection of immunocompetent BALB/c mice with this dose of IL-13 enhances worm expulsion (15). All mice were studied 7 days after the initial injection.

Nematode infection

Infective, third-stage larvae of *N. brasiliensis* (L3; specimens on file at the U.S. National Parasite Collection, U.S. National Helminthological Collection, Collection 81930) were propagated and stored at room temperature in fecal/charcoal/peat moss culture plates until used. WT, STAT6$^{-/-}$, IL-4$^{-/-}$, or IL-13$^{-/-}$ mice were inoculated s.c. with 500 *N. brasiliensis* L3 and studied 9 days later. Appropriate age-matched controls were used for each infection.

In vitro contractility

One-centimeter segments of jejunum were flushed of their intestinal contents, suspended longitudinally in individual 8-ml organ baths, and maintained in oxygenated Krebs solution at 37°C. One end of the tissue was attached to an isometric tension transducer (model FT03; Grass Medical Instruments), and the other to the bottom of the bath. Tissues were stretched to a load of 9.9 mN (2 g). Preliminary experiments showed that this load stretched tissues to their optimal length for active contraction. Tissues were allowed to equilibrate for at least 30 min in Krebs buffer solution before study, and the bath solution was replaced every 10 min. Tension was recorded using a Grass model 79 polygraph and was expressed as force per cross-sectional area (16). After equilibration, the frequency and amplitude of the spontaneous, rhythmic contractions that occur in the absence of any stimulation were measured over a 2-min period. Tissues were then challenged with thrombin (10 nM to 10 μM) or with the PAR-1-activating peptide, TFLLR (1–100 μM). The reverse amino acid sequence peptide, RLLFT, or boiled thrombin (100°C for 5 min) was used as the control for TFLLR and thrombin, respectively. Because of the potential for PAR-1 desensitization, thrombin was applied only once, and TFLLR only twice, to each tissue preparation, with a 60-min interval between the two challenges. Preliminary data showed that a 60-min interval allowed for the complete restoration of responses to TFLLR. To compare the responses to PAR-1 agonist among different groups of mice, intestinal strips were challenged at a single time with 100 μM TFLLR.

Gastrointestinal (GI) transit

To determine whether *N. brasiliensis*-induced changes in contractility in mice also altered GI transit, fasted conscious mice ($n = 5$/group) were given 0.2 ml of ^{51}Cr (5 μCi/ml) by oral gavage (17). Mice were killed after 25 min, because it has been shown that the bulk of the marker was distributed along the small intestine at this time point. The small intestine was removed, divided into 10 equally sized parts, and, along with the stomach, placed in individual tubes and counted for gamma activity in a Beckman 4000 gamma counter (Beckman Coulter). Values were corrected for background and counts in each segment. Counts were expressed as a percentage of the total counts in the small intestine, thereby removing the effect of any variability of gastric emptying and allowing the specific determination of intestinal transit. Changes in transit between uninfected and *N. brasilensis*-infected groups were assessed using two parameters. First, the amount of activity in the final segment of the intestine (leading edge) was used as an index of total movement of the marker. Second, the geometric center was calculated to determine the overall distribution of the marker, which is used as an index of the overall propulsive activity along the intestine (17): Σ[(counts in segment/total intestinal counts) × segment no.].

RNA extraction and cDNA synthesis

Total RNA was extracted with TRIzol reagent (Invitrogen Life Technologies) according to the manufacturer's instructions. RNA integrity, quantity, and genomic DNA contamination were assessed using the Bioanalyzer 2100 and RNA 6000 Labchip kit (Agilent Technologies). Only those RNA samples with 28S/18S ratios between 1.5 and 2 and no DNA contamination were studied further. RNA samples (2 μg) were reverse transcribed to cDNA using the First Strand cDNA Synthase kit (MBI Fermentas) with random hexamer primer (18).

Real-time quantitative PCR

Real-time PCR was performed with a PRISM 7700 sequence detection system (Applied Biosystems). Primer and probe sequences were designed using computer program Primer Express 1.5 (Applied Biosystems) and were synthesized by BioSource International. The following primers and probes were used: PAR-1, 5′-GCTGGAGGGTAGGGCAGTCT (sense), 5′-GTACACGGAGGGCATGAAGAG (antisense), and 5′-CTCCCTTCATCTCCGAGGACGCCT (probe); IL-4, 5′-CGGAGATGGATGTGCCAAAC (sense), 5′-GCACCTTGGAAGCCCTACAG (antisense), and 5′-TCCTCACAGCAACGAAGAACACCACA (probe); and IL-13, 5′-GACCAGACTCCCCTGTGCAA (sense), 5′-TGGGTCCTGTAGATGGCATTG (antisense), and 5′-CGGGTTCTGTGTAGCCCTGGATTCC (probe).

PCR was performed in a 25-μl volume using a Brilliant Quantitative PCR Core Reagent kit (Stratagene). Assays were optimized as follows. Primer and probe concentrations were varied until the highest signal intensity and the lowest threshold of detection were achieved; cDNA templates were diluted to determine linearity of optimum primer and probe concentration. Amplification conditions were 50°C for 2 min, 95°C for 10 min, and 40 cycles of 95°C for 15 s and 60°C for 1 min. The fold changes in mRNA expression for PAR-1, IL-4, and IL-13 were relative to the respective vehicle groups of mice after normalization to 18S rRNA (Applied Biosystems).

Immunofluorescent staining

Frozen blocks of midjejunum were prepared by using the Swiss roll technique and were stored at −80°C. Tissue sections (4 μm) were cut from frozen blocks using an HM505E cryostat (Richard Allan Scientific). Slides were kept on dry ice and then stored at −80°C. For immunofluorescent staining, tissue slides were fixed in cold acetone for 30 min and blocked with 10% normal goat serum in PBS for 1 h at room temperature. The slides were incubated with anti-PAR-1 (1/50; Santa Cruz Biotechnology) overnight in a humidified chamber at 4°C, followed by incubation with avidin-Alexa Fluor 488 (1/200; Molecular Probes). The slides were then coverslipped with Vectorshield (Vector Laboratories) and digitally photographed with a Nikon E800 microscope using Nikon DXM 1200 software. The intensity of staining was determined by establishing settings for the samples from the individual vehicle groups and using the same conditions to evaluate the samples from the infected or treated groups. Comparisons were made only among the slides prepared on the same day.

Solutions and drugs

Krebs buffer contained 4.74 mM KCl, 2.54 mM $CaCl_2$, 118.5 mM NaCl, 1.19 mM NaH_2PO_4, 1.19 mM $MgSO_4$, 25.0 mM $NaHCO_3$, and 11.0 mM glucose. All drugs were obtained from Sigma-Aldrich unless indicated otherwise. Stock solutions were prepared as follows. Thrombin (1 mM) was dissolved in distilled water. The PAR-1 peptide agonist, TFLLR; the inactive reverse amino acid sequence peptide, RLLFT; and two PAR-3/PAR-4 peptide agonists, SFNGGP and AYPGKF (10 mM; synthesized by University Biomedical Instrumentation Center), were dissolved in 20% DMSO, and stored at −70°C in aliquots. On the day of the experiment, appropriate dilutions of thrombin and the peptides were made using distilled water.

Data analysis

Agonist responses were fitted to sigmoid curves (GraphPad). Statistical analysis was performed using one-way ANOVA, followed by Tukey's test to compare the responses and mRNA expression among the different treatment groups. Appropriate vehicle-treated and time- and age-matched controls were performed for each group.

Results

PAR-1 agonists elicit a concentration-dependent contraction of intestinal smooth muscle

To evaluate the effect of PAR-1 activation on intestinal longitudinal smooth muscle contractility, we applied thrombin to a segment of jejunum from untreated WT mice. Thrombin evoked a small relaxation, followed by a sustained, concentration-dependent contraction (Fig. 1). The small relaxation was independent of thrombin concentration and was observed in most tissue strips (~90%). Boiled thrombin had no effect (data not shown). Because thrombin activates PAR-3 and PAR-4 in addition to PAR-1, we then used a more specific PAR agonist to determine the PAR-1 dependence of the thrombin-induced increase in contractility. The PAR-1-specific peptide, TFLLR, induced a similar response to thrombin (Fig. 1). The amplitude of the contraction induced by 10 μM TFLLR was also similar to that induced by 1 mM acetylcholine (10,730 ± 1,350 vs 9,927 ± 1,228 mN/cm^2), a major excitatory neurotransmitter in the gut, and to that induced by 1 μM substance P (10,730 ± 1,350 vs 11,589 ± 1,017 mN/cm^2), a sensory neurotransmitter. In contrast, the PAR-3- and PAR-4-activating peptides, SFNGGP and AYPGKF; the PAR-1 reverse peptide, RLLFT; and vehicle (20% DMSO) had no effect on small intestinal contractility (data not shown). These data indicate that the major effect of thrombin is via activation of PAR-1.

N. brasiliensis infection increases intestinal smooth muscle responses to a PAR-1 agonist by STAT6-dependent up-regulation of PAR-1 expression

As shown previously, *N. brasiliensis* infection induced intestinal smooth muscle hypercontractility (12) that was characterized by increased responses to acetylcholine, nerve stimulation, and substance P. *N. brasiliensis* also increased the amplitude of spontaneous intestinal smooth muscle contractions (Table I) without affecting their frequency. Because PAR-1 agonists contract intestinal smooth muscle, we evaluated whether *N. brasiliensis* infection affects PAR-1 agonist-evoked contractions and correlated functional changes with the expression of PAR-1 mRNA and protein levels. *N. brasiliensis* infection induced a significant increase in smooth muscle responses to TFLLR (Fig. 2*A*) along with an ~3-fold up-regulation of PAR-1 mRNA expression (Fig. 2*B*) and increased intensity of staining for PAR-1 in mouse intestine. This increase in staining intensity was especially evident in intestinal smooth muscle (Fig. 3, *A* and *B*).

Because *N. brasiliensis* infection-induced hypercontractility depends on STAT6 (12), we compared responses to PAR-1 agonists in infected and uninfected WT and STAT6$^{-/-}$ mice. Intestinal smooth muscle hypercontractility and increases in PAR-1 mRNA and protein expression failed to develop in *N. brasiliensis*-infected STAT6$^{-/-}$ mice (Table I and Figs. 2 and 3). Thus, helminth-induced hypercontractility to PAR-1 activation and up-regulation of PAR-1 mRNA and protein expression were uniformly dependent on activation of STAT6. This STAT6 dependence was not a reflection of STAT6 dependence of IL-4/IL-13 expression, which was elevated to the same extent in *N. brasiliensis*-infected STAT6$^{-/-}$ and WT mice (Table II).

N. brasiliensis infection produced subtle changes in GI transit. Uninfected mice showed a consistent pattern of marker distribution, with a clear peak in segment 8 (22% of the marker). In contrast, *N. brasiliensis* infection produced an even distribution of the marker along the GI tract, with no clear peak. As a result, infection did not alter the geometric center significantly (4.7 ± 0.3 vs 5.6 ± 0.4; $p = 0.09$), but significantly increased the percentage of the marker in the most distal segment of the small intestine (0.6 ± 0.3 vs 7.8 ± 3.0; $p < 0.01$).

N. brasiliensis infection-induced changes in responses to PAR-1 activation as well as up-regulation of PAR-1 expression are mediated by IL-13, not by IL-4

N. brasiliensis infection dramatically elevates systemic levels of the Th2 cytokines, IL-4 and IL-13 (15), and significantly enhances tissue IL-4 and IL-13 levels in the small intestine (Table II). Because the helminth-induced increases in PAR-1 expression in WT mice were absent in STAT6$^{-/-}$ mice, we next determined the contributions of IL-4 and IL-13 to the up-regulation of PAR-1 activity by comparing spontaneous contractions; responses to the PAR-1 agonist, TFLLR; and expression of PAR-1 in small intestine of *N. brasiliensis*-infected IL-4$^{-/-}$ and IL-13$^{-/-}$ mice. The infection-induced increased amplitude of spontaneous contractions and hypercontractility to the PAR-1 agonist, TFLLR, in WT mice was not observed in *N. brasiliensis*-infected IL-13$^{-/-}$ mice (Table I and Fig. 4A), indicating a dependence on IL-13. Coincident with the smooth muscle response to TFLLR, there were no changes in PAR-1 mRNA expression (Fig. 4*B*) or immunofluorescent staining of PAR-1 in intestinal smooth muscle after infection in IL-13$^{-/-}$ mice (Fig. 5, *C* and *D*). In contrast, the amplitude of spontaneous contraction (Table I) and responses to a PAR-1 agonist (Fig. 4*A*) in infected IL-4$^{-/-}$ mice were similar to those in infected WT mice, as were increases in PAR-1 mRNA expression (Fig. 4*B*) and immunofluorescent staining of PAR-1 (Fig. 5, *A* and *B*). Importantly, *N. brasiliensis* increased IL-13 expression in IL-4$^{-/-}$ mice, although less than in WT mice, indicating that the effects of IL-13 on PAR-1 are evident even at relatively low levels of expression, whereas IL-4 expression was increased to the same extent in WT and IL-13$^{-/-}$ (Table II). Thus, up-regulation of IL-13, rather than IL-4, is responsible for the increased PAR-1 expression and response to PAR-1 activation in the small intestine of *N. brasiliensis*-infected mice.

Administration of IL-13 induced a STAT6-dependent increase in PAR-1 expression and smooth muscle responses to a PAR-1 agonist

To define the contribution of IL-13 to *N. brasiliensis*-induced changes in PAR-1 activity and expression, mice were injected with IL-13 for 7 days. As shown previously, IL-13 induced intestinal smooth muscle hypercontractility (12) and increased the amplitude of the spontaneous contraction of intestinal smooth muscle strips (Table I). IL-13 also increased smooth muscle responses to TFLLR (Fig. 2*A*) and up-regulated the expression of PAR-1 mRNA (Fig. 2*B*) and protein (Fig. 3, *A* and *C*). In contrast, IL-13 failed to induce smooth muscle hypercontractility or increased PAR-1 expression in STAT6$^{-/-}$ mice (Fig. 2, *A* and *B*, and Fig. 3, *D* and *F*). Thus, the effects of IL-13 on PAR-1 activity and expression are STAT6 dependent.

Discussion

The present study is the first to demonstrate immune regulation of both PAR-1 activity and expression. The three major findings to emerge from this study are that helminth infection-induced alterations in PAR-1 expression are dependent on IL-13 and STAT6, that the immune-mediated changes in PAR-1 expression have a functional correlate, and that the enhanced smooth muscle responses to PAR-1 agonists are associated with an increased number of receptors.

Serine proteases, the potential physiological agonists of PARs, are present in significant quantities in the lumen of the small intestine, and their presence is linked to a number of pathological processes, including inflammation (1). The large numbers of cells identified within the intestinal wall that express PAR-1 suggest that the proteases may also act as signaling molecules and play a role in the regulation of intestinal function (2). Thrombin, the endogenous ligand of PAR-1, exhibits both proinflammatory effects (vascular permeability and

chemotaxis) and protective mucosal changes (tissue repair and wound healing), suggesting a role for PAR-1 activation in host defense.

The intestine is an important immune interface, and polarized cytokines profiles produced by Th1 and Th2 cells are integral to the coordination of immune and nonimmune cell interactions that mediate protection against enteric pathogens. Infection of mice with intestinal nematode parasites, such as *N. brasiliensis*, induces a strong Th2 cytokine response required for worm expulsion (15). Clearance is associated with changes in intestinal physiology, including smooth muscle hypercontractility (12). There is evidence that PARs play a critical role in the constitutive modulation of motility of the gastrointestinal smooth muscle (19). We show in this study that *N. brasiliensis* infection increased intestinal smooth muscle responses to a PAR-1 agonist and up-regulated PAR-1 expression. A major consideration in defining a role for PARs is that after activation, PARs undergo rapid internalization, and most are targeted for lysosomal degradation. Because receptors must be recycled to the surface, graded responses to PARs depend on the rate of receptor cleavage, which may limit the magnitude and/or duration of their effects under physiological conditions (5). Key factors in the cellular response to proteases, therefore, are the number of receptors and the presence of intracellular stores that can rapidly replenish surface receptors. In the present study, PAR-1-positive staining is visible throughout the section in control mice; however, the greater intensity of staining in the smooth muscle layer from infected mice is compatible with the possibility that the infection-induced hypercontractility to PAR-1 agonists is due to an increased number of receptors in smooth muscle.

PAR-1 activation in vivo increases intestinal transit (11), suggesting that this may be a mechanism by which PAR-1 contributes to worm expulsion. Previous studies indicate that nematode infection generally promotes GI transit. Early reports show that a radioactive marker transversed 100% of the gut length in *Trichinella spiralis*-infected rats and 70% in controls (20). Others showed that intestinal propulsive activity was increased significantly on day 8 after *N. brasiliensis* infection, yet overall intestinal transit was unchanged from controls on days 6, 10, 12, and 14 after infection, suggesting that the changes in transit may be transient (21). It is interesting that there is an enhanced contractility on day 9 in the present study as well as on day 7 after infection (our unpublished observations), indicating that hypercontractility is not necessarily associated with increased transit. Other in vivo correlates of increased in vitro contractility in helminth-infected mice may be the disrupted normal migrating motor patterns (22), the appearance of atypical giant migrating contractions associated with increased fluid in the intestine (23), or the loss of extrinsic input from the vagus (24). These data suggest that the *N. brasiliensis*-induced hypercontractility may be linked to alterations in several different motor patterns events, all of which contribute to worm expulsion, and that PAR-1 activation is probably one of several mechanisms that contribute to *N. brasiliensis* expulsion.

Previous studies showed that the changes in intestinal smooth muscle function induced by *N. brasiliensis* infection are dependent on the production of Th2 cytokines. Levels of IL-4 and IL-13 production are elevated dramatically in the small intestine and mesenteric lymph node during *N. brasiliensis* infection. IL-4 and IL-13 enhance smooth muscle contractility, and both bind to the type 2 IL-4R (IL-4Rα/IL-13Rα1) that is linked to the STAT6 signaling pathway. The increased response to a PAR-1 agonist and the up-regulation of PAR-1 expression in intestinal smooth muscle were absent in $STAT6^{-/-}$ mice, indicating that PAR-1-induced hypercontractility in *N. brasiliensis* infection is STAT6 dependent. Thrombin activates JAK2, which is linked to STAT2 and STAT4 signaling in vascular smooth muscle cells (25); thus, it is conceivable that PAR-1 also acts through JAK pathways linked to STAT6.

To determine the contributions of IL-4 and IL-13, we studied the effects of *N. brasiliensis* infection on PAR-1 in mice deficient in either IL-4 or IL-13. IL-4 is believed to be the central

differentiation factor for Th2 response development. The increased response to the PAR-1 agonist, TFLLR, and the up-regulation of PAR-1 expression were retained in *N. brasiliensis*-infected IL-4$^{-/-}$ mice, indicating that IL-4 is not necessary for *N. brasiliensis*-induced changes in responses to PAR-1. In contrast, the enhanced response to PAR-1 in *N. brasiliensis* infection was absent in IL-13-deficient mice despite elevated production of IL-4. Furthermore, PAR-1 responses and expression were enhanced similarly in WT mice treated with exogenous IL-13 or infected with *N. brasiliensis* and were not observed in STAT6$^{-/-}$ mice. Previous studies showed that *N. brasiliensis* clearance in IL-4$^{-/-}$ mice was normal, but was impaired in IL-13$^{-/-}$ mice (15,26). Our current findings are consistent with the observation that IL-13 plays a major role in the host response to *N. brasiliensis*. Mastocytosis is an important feature of the Th2 response, but is not required for clearance of *N. brasiliensis*. Mast cells release a number of serine proteases that could activate PAR-2; however, thrombin, the endogenous ligand of PAR-1, is not considered to be a product of mast cells. We showed previously that IL-4, but not IL-13, induced mastocytosis (13) that was dependent in part on STAT6. In the present study the increased response to and the expression of PAR-1 after *N. brasiliensis* infection are linked to IL-13, rather than to IL-4. This reliance on IL-13 indicates that mast cells may not be important in the PAR-1-mediated effects on smooth muscle contractility.

The immune regulation of PAR-1 activity and expression via IL-13 has a number of implications. Both *N. brasiliensis* infection and IL-13 induce a hypercontractility of intestinal smooth muscle (12). Liver fibrosis resulting from *Schistosoma mansoni* infection as well as the airway hyperactivity in asthma are mediated primarily by IL-13 (27,28). Moreover, IL-13 is a potent stimulator of C10/cCCL6, and its signaling through the receptor, CCR1, is linked to IL-13-induced proteases and chemokines in the lung (29). Similarly, PAR-1 is also present within the respiratory tract, where it is linked to pulmonary fibrosis (30). Furthermore, activation of PAR-1 stimulates the proliferation of vascular smooth muscle cells (31), and up-regulation of PAR-1 expression in both vascular and intestinal smooth muscles in response to irradiation has been proposed to contribute to radiation fibrosis (32). These data indicate that both IL-13 and PAR-1 are involved in tissue remodeling and fibrosis in a number of organ systems and suggest that their interaction may provide an important therapeutic target. Unregulated fibrosis or smooth muscle hypertrophy/hyperplasia in the small intestine is a characteristic of intestinal obstruction as well as inflammation and would also interfere with intestinal absorption and transit. Tight control is critical to promote the resolution of transient changes, which may benefit the host, and to prevent progression into long term changes associated with chronic disease.

In summary, *N. brasiliensis* infection induced smooth muscle hypercontractility in response to PAR-1 agonist and up-regulated PAR expression in murine small intestine. These effects are mediated primarily by IL-13, are dependent on STAT6, and are specific to smooth muscle. This is the first report to link IL-13 and a PAR, each of which has been implicated in a variety of pathologies. The immune regulation of PAR-1 actions on smooth muscle represents a novel therapeutic target in the modulation of IL-13 effector activity, given that many reactive allergens and helminth excretory/secretory products contain protease moieties that could enhance PAR-1 activation.

Acknowledgements

We thank Dr. Debra Donaldson (Respiratory Disease, Wyeth Research, Cambridge, MA) for the generous gift of IL-13.

This work was supported by National Institutes of Health Grants RO1AI/DK49316 (to T.S.-D.) and R01AI35987 and R01AI052099 (to F.D.F.), and U.S. Department of Agriculture CRIS Project 1235-52000-053. The opinions and assertions in this article are those of the authors and do not necessarily represent those of the U.S. Department of Defense or the U.S. Department of Agriculture.

References

1. Macfarlane SR, Seatter MJ, Kanke T, Hunter GD, Plevin R. Proteinase-activated receptors. Pharmacol Rev 2001;53:245–282. [PubMed: 11356985]
2. Vergnolle N. Review article: proteinase-activated receptors-novel signals for gastrointestinal pathophysiology. Aliment Pharmacol Ther 2000;14:257–266. [PubMed: 10735917]
3. Schmidlin F, Bunnett NW. Protease-activated receptors: how proteases signal to cells. Curr Opin Pharmacol 2001;1:575–582. [PubMed: 11757812]
4. Vu TK, Hung DT, Wheaton VI, Coughlin SR. Molecular cloning of a functional thrombin receptor reveals a novel proteolytic mechanism of receptor activation. Cell 1991;64:1057–1068. [PubMed: 1672265]
5. Ossovskaya VS, Bunnett NW. Protease-activated receptors: contribution to physiology and disease. Physiol Rev 2003;84:579–621. [PubMed: 15044683]
6. Buresi MC, Buret AG, Hollenberg MD, MacNaughton WK. Activation of proteinase-activated receptor 1 stimulates epithelial chloride secretion through a unique MAP kinase- and cyclo-oxygenase-dependent pathway. FASEB J 2002;16:1515–1525. [PubMed: 12374774]
7. Buresi MC, Schleihauf E, Vergnolle N, Buret A, Wallace JL, Hollenberg MD, MacNaughton WK. Protease-activated receptor-1 stimulates Ca^{2+}-dependent Cl^{-} secretion in human intestinal epithelial cells. Am J Physiol 2001;281:G323–G332.
8. Kawabata A, Saifeddine M, Al-Ani B, Leblond L, Hollenberg MD. Evaluation of proteinase-activated receptor-1 (PAR1) agonists and antagonists using a cultured cell receptor desensitization assay: activation of PAR2 by PAR1-targeted ligands. J Pharmacol Exp Ther 1999;288:358–370. [PubMed: 9862790]
9. Cocks TM, Sozzi V, Moffatt JD, Selemidis S. Protease-activated receptors mediate apamin-sensitive relaxation of mouse and guinea pig gastrointestinal smooth muscle. Gastroenterology 1999;116:586–592. [PubMed: 10029617]
10. Mule F, Baffi MC, Cerra MC. Dual effect mediated by protease-activated receptors on the mechanical activity of rat colon. Br J Pharmacol 2002;136:367–374. [PubMed: 12023939]
11. Kawabata A, Kuroda R, Nagata N, Kawao N, Masuko T, Nishikawa H, Kawai K. In vivo evidence that protease-activated receptors 1 and 2 modulate gastrointestinal transit in the mouse. Br J Pharmacol 2001;133:1213–1218. [PubMed: 11498505]
12. Zhao A, McDermott J, Urban JF Jr, Gause WC, Madden KB, Yeung KA, Morris SC, Finkelman FD, Shea-Donohue T. Dependence of IL-4, IL-13, and nematode-induced alterations in murine small intestinal smooth muscle contractility on Stat6 and enteric nerves. J Immunol 2003;171:948–954. [PubMed: 12847266]
13. Madden KB, Whitman L, Sullivan C, Gause WC, Urban JF Jr, Katona IM, Finkelman FD, Shea-Donohue T. Role of STAT6 and mast cells in IL-4- and IL-13-induced alterations in murine intestinal epithelial cell function. J Immunol 2002;169:4417–4422. [PubMed: 12370375]
14. Finkelman FD, Shea-Donohue T, Goldhill J, Sullivan CA, Morris SC, Madden KB, Gause WC, Urban JF Jr. Cytokine regulation of host defense against parasitic gastrointestinal nematodes: lessons from studies with rodent models. Annu Rev Immunol 1997;15:505–533. [PubMed: 9143698]
15. Urban JF Jr, Noben-Trauth N, Donaldson DD, Madden KB, Morris SC, Collins M, Finkelman FD. IL-13, IL-4Rα, and Stat6 are required for the expulsion of the gastrointestinal nematode parasite *Nippostrongylus brasiliensis*. Immunity 1998;8:255–264. [PubMed: 9492006]
16. Zhao A, Bossone C, Pineiro-Carrero V, Shea-Donohue T. Colitis-induced alterations in adrenergic control of circular smooth muscle in vitro in rats. J Pharmacol Exp Ther 2001;299:768–774. [PubMed: 11602693]
17. Shook JE, Pelton JT, Hruby VJ, Burks TF. Peptide opioid antagonist separates peripheral and central opioid antitransit effects. J Pharmacol Exp Ther 1987;243:492–500. [PubMed: 2824748]
18. Dawson HD, Royaee AR, Nishi S, Kuhar D, Schnitzlein WM, Zuckermann F, Urban JF Jr, Lunney JK. Identification of key immune mediators regulating T helper 1 responses in swine. Vet Immunol Immunopathol 2004;100:105–111. [PubMed: 15183000]
19. Zhao A, Shea-Donohue T. PAR-2 agonists induce contraction of murine small intestine through neurokinin receptors. Am J Physiol 2003;285:G696–G703.

20. Castro GA, Badial-Aceves F, Smith JW, Dudrick SJ, Weisbrodt NW. Altered small bowel propulsion associated with parasitism. Gastroenterology 1976;71:620–625. [PubMed: 955350]
21. Farmer SG. Propulsive activity of the rat small intestine during infection with the nematode *Nippostrongylus brasiliensis*. Parasite Immunol 1981;3:227–234. [PubMed: 7301408]
22. Palmer JM, Greenwood-Van Meerveld B. Integrative neuroimmunomodulation of gastrointestinal function during enteric parasitism. J Parasitol 2001;87:483–504. [PubMed: 11426710]
23. Cowles VE, Sarna SK. Effect of T. spiralis infection on intestinal motor activity in the fasted state. Am J Physiol 1990;259:G693–G701. [PubMed: 2240213]
24. Venkova K, Palmer JM, Greenwood-Van Meerveld B. Nematode-induced jejunal inflammation in the ferret causes long-term changes in excitatory neuromuscular responses. J Pharmacol Exp Ther 1999;290:96–103. [PubMed: 10381764]
25. Madamanchi NR, Li S, Patterson C, Runge MS. Thrombin regulates vascular smooth muscle cell growth and heat shock proteins via the JAK-STAT pathway. J Biol Chem 2001;276:18915–18924. [PubMed: 11278437]
26. McKenzie GJ, Bancroft A, Grencis RK, McKenzie AN. A distinct role for interleukin-13 in Th2-cell-mediated immune responses. Curr Biol 1998;8:339–342. [PubMed: 9512421]
27. Chiaramonte MG, Cheever AW, Malley JD, Donaldson DD, Wynn TA. Studies of murine schistosomiasis reveal interleukin-13 blockade as a treatment for established and progressive liver fibrosis. Hepatology 2001;34:273–282. [PubMed: 11481612]
28. Wynn TA. IL-13 effector functions. Annu Rev Immunol 2003;21:425–456. [PubMed: 12615888]
29. Ma B, Zhu Z, Homer RJ, Gerard C, Strieter R, Elias JA. The C10/cCCL6 chemokine and CCR1 play critical roles in the pathogenesis of IL-13-induced inflammation and remodeling. J Immunol 2004;172:1872–1881. [PubMed: 14734772]
30. Tran T, Stewart AG. Protease-activated receptor (PAR)-independent growth and pro-inflammatory actions of thrombin on human cultured airway smooth muscle. Br J Pharmacol 2003;138:865–875. [PubMed: 12642388]
31. McNamara CA, Sarembock IJ, Gimple LW, Fenton JW Jr, Coughlin SR, Owens GK. Thrombin stimulates proliferation of cultured rat aortic smooth muscle cells by a proteolytically activated receptor. J Clin Invest 1993;91:94–98. [PubMed: 8380817]
32. Wang J, Zheng H, Ou X, Fink LM, Hauer-Jensen M. Deficiency of microvascular thrombomodulin up-regulation of protease-activated receptor-1 in irradiated rat intestine: possible link between endothelial dysfunction and chronic radiation fibrosis. Am J Pathol 2002;160:2063–2072. [PubMed: 12057911]

Abbreviations used in this paper

PAR
protease-activated receptor

GI
gastrointestinal

WT
wild type

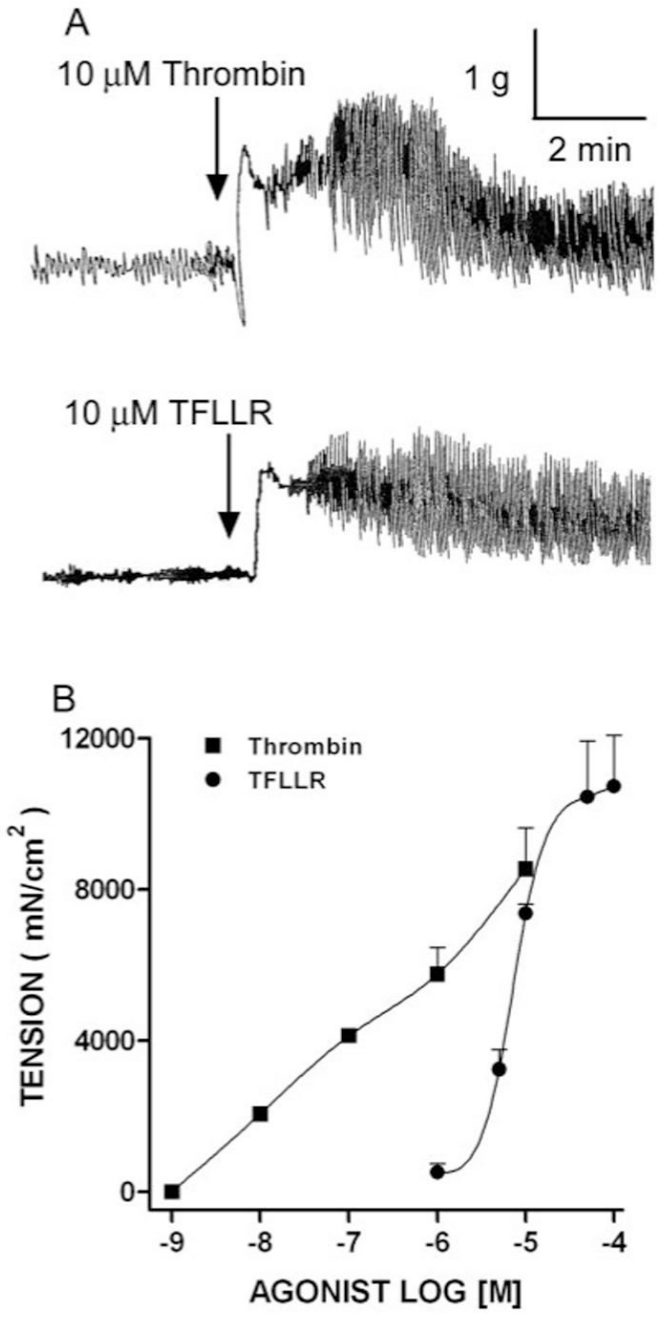

FIGURE 1.

PAR-1 agonists evoked contractions of untreated control murine small intestinal smooth muscle. *A*, Tracings of thrombin or TFLLR (10 μM)-evoked contractions. Each tracing is representative of at least four independent experiments. *B*, Thrombin or TFLLR induced concentration-dependent contraction curves of intestinal smooth muscle.

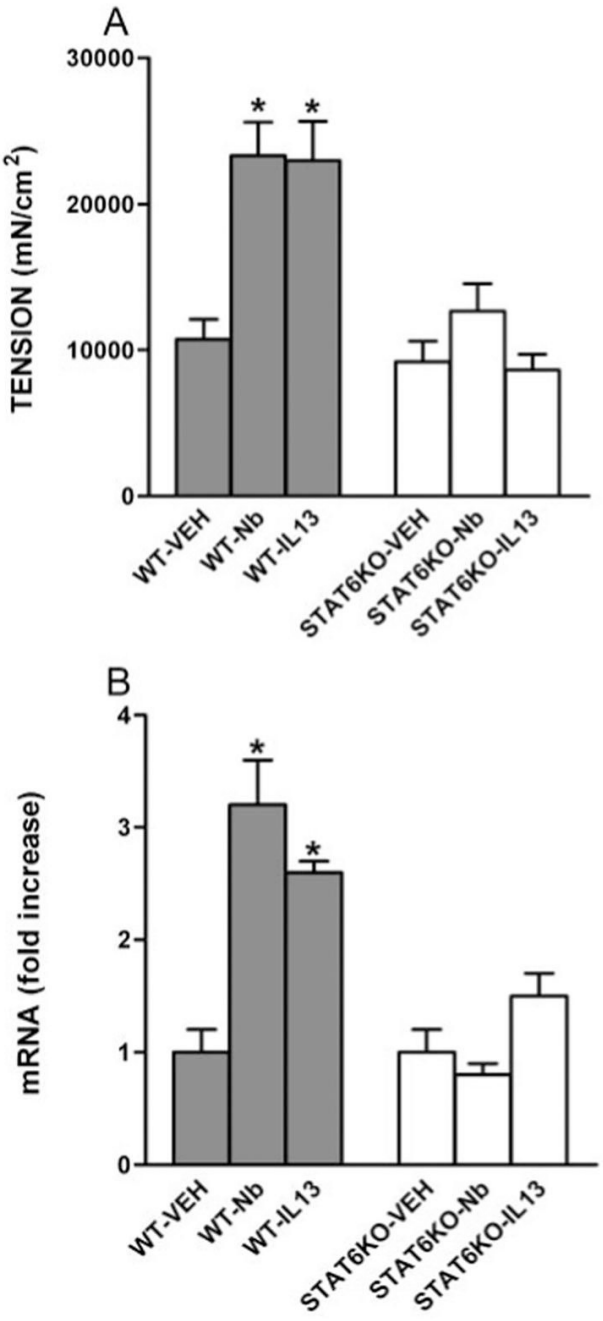

FIGURE 2.

Effects of *N. brasiliensis* (Nb) infection on PAR-1 responsiveness and expression by intestine from WT or STAT6-deficient (STAT6 KO) mice. Mice were injected i.v. with IL-13 daily for 7 days or with an equal volume of normal saline (VEH), inoculated s.c. with 500 *N. brasiliensis* infective third-stage larvae (L3), and studied 9 days later. Intestinal strips were taken from the mice and suspended longitudinally in organ baths for in vitro contractility studies in response to 100 μM of the PAR-1 agonist, TFLLR (*A*), or for total RNA extraction (*B*). After RT, real-time PCR was performed to measure PAR-1 mRNA expression. The fold increases were relative to the individual vehicle groups after normalization to 18S rRNA. *, $p < 0.05$ compared with WT-VEH ($n \geq 4$ for each group).

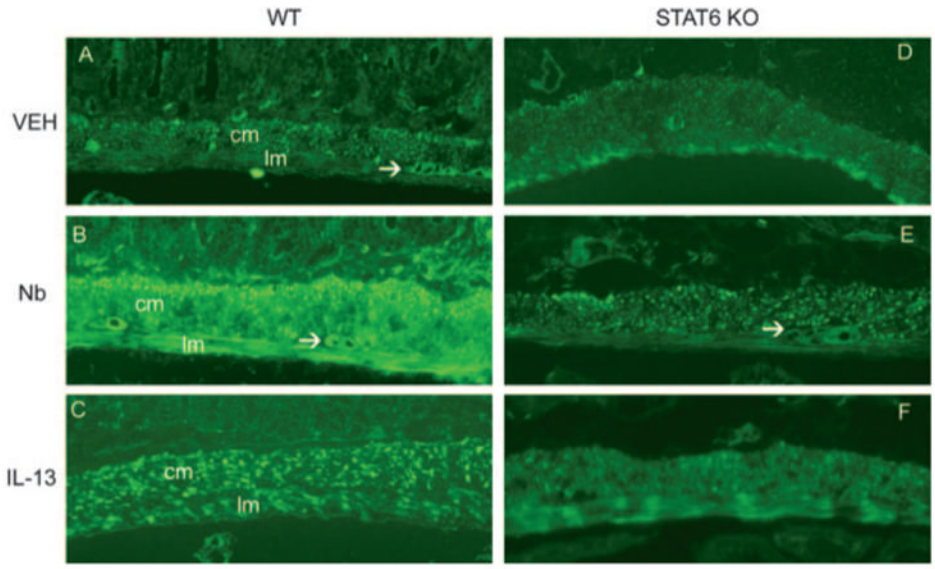

FIGURE 3.

PAR-1 expression was increased by IL-13 or *N. brasiliensis* (Nb) infection in the intestines from WT, but not STAT6-deficient (STAT6 KO), mice. WT (*A–C*) or STAT6-deficient mice (*D–F*) were injected i.v. with IL-13 daily for 7 days or with an equal volume of normal saline (VEH), inoculated s.c. with 500 *N. brasiliensis* infective third-stage larvae (L3), and studied 9 days later. Frozen tissue blocks of midjejunum were prepared, and the sections were cut for immunofluorescence staining for PAR-1. The intensity of the staining was determined by establishing settings for the samples from the individual vehicle groups and using the same conditions to evaluate the samples from the infected or treated groups. PAR-1-positive staining is visible throughout the section and is most prominent in smooth muscle layer, including circular (cm) and longitudinal (lm) smooth muscle, and the myenteric neurons (arrows). As the negative controls, the sections incubated with normal rabbit IgG or secondary Ab only showed no staining (not shown). One representative picture from each group of at least four mice is shown. Magnification, ×100.

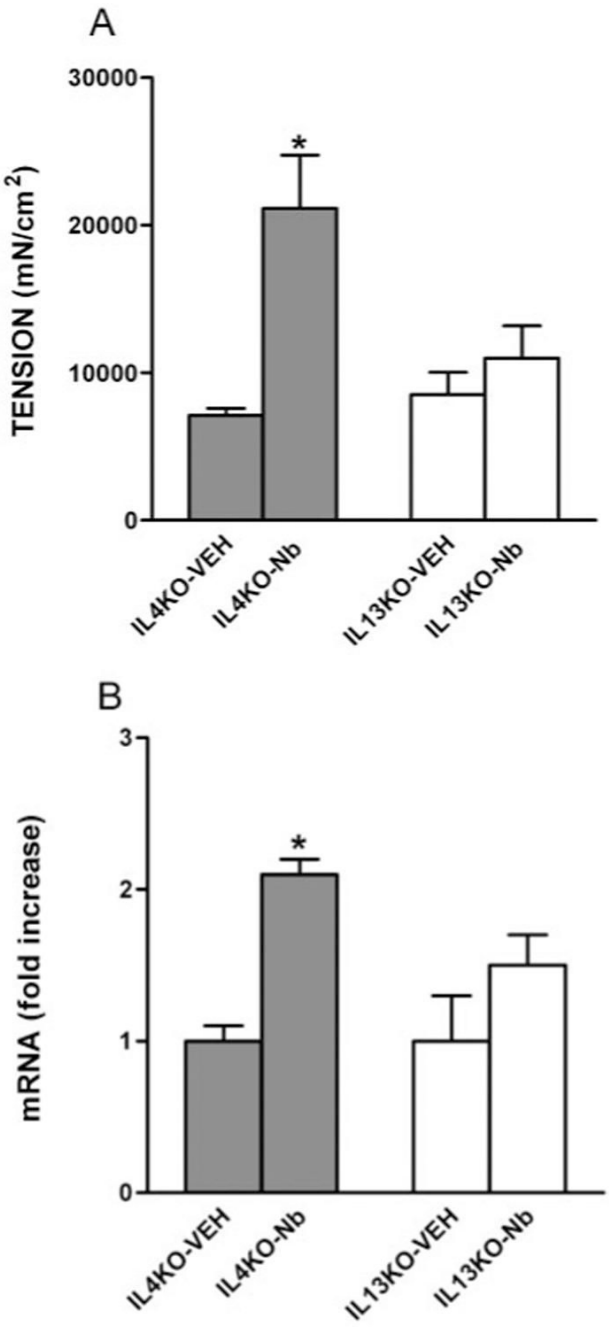

FIGURE 4.

Effects of *N. brasiliensis* (Nb) infection on PAR-1 responsiveness and expression by intestines from IL-4-deficient (IL-4 KO) or IL-13-deficient (IL-13 KO) mice. Mice were inoculated s.c. with 500 *N. brasiliensis* infective third-stage larvae (L3) or vehicle (VEH) and were studied 9 days later. Intestinal strips were suspended longitudinally in organ baths for in vitro contractility studies in response to 100 μM of the PAR-1 agonist, TFLLR (*A*), or were extracted for total RNA (*B*). After RT, real-time PCR was performed to measure PAR-1 mRNA expression. The fold increases were relative to the individual vehicle group after normalization to 18S rRNA. *, $p < 0.05$ compared with IL-4KO-VEH ($n \geq 4$ for each group).

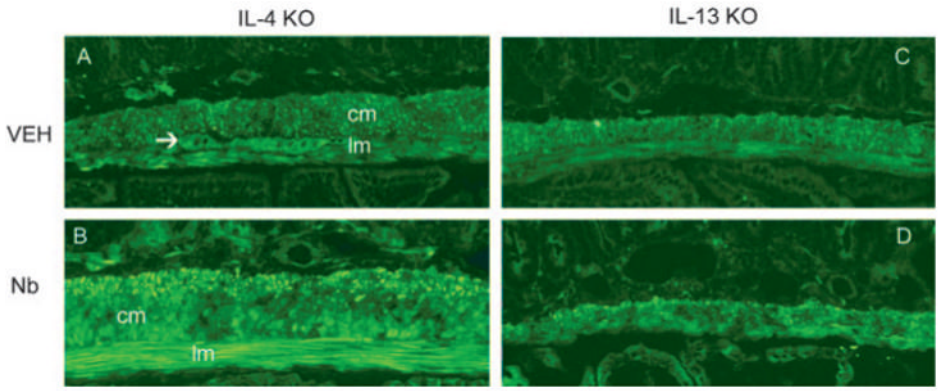

FIGURE 5.

PAR-1 expression was increased by *N. brasiliensis* (Nb) infection in the intestines from IL-4-deficient (IL-4 KO), but not IL-13-deficient (IL-13 KO), mice. Mice were inoculated s.c. with 500 *N. brasiliensis* infective third-stage larvae (L3) or were treated with vehicle (VEH) and studied 9 days later. Frozen tissue blocks of midjejunum were prepared, and the sections were cut for immunofluorescence staining for PAR-1. The intensity of the staining was determined by establishing settings for the samples from the individual vehicle groups and using the same conditions to evaluate the samples from the infected or treated groups. PAR-1-positive staining is visible throughout the section and is most prominent in smooth muscle layer, including circular (cm) and longitudinal (lm) smooth muscles, and the myenteric neurons (arrows). As the negative controls, the sections incubated with normal rabbit IgG or secondary Ab only showed no staining (not shown). One representative picture from each group of at least four mice is shown. Magnification, ×100.

Table I

Amplitude of spontaneous contractions of intestinal longitudinal smooth muscle from mice treated/infected with vehicle, IL-13, or *N. brasiliensis*[a]

Mice	Vehicle	IL-13 Injected	*Nb* infected
Wild type	4,431 ± 644	9,694 ± 1,318*	10,747 ± 1,453*
Stat6$^{-/-}$	3,623 ± 495	3,323 ± 379	4,417 ± 582
IL-13$^{-/-}$	2,693 ± 207	ND	2,820 ± 325
IL-4$^{-/-}$	4,074 ± 904	ND	9,539 ± 1,284*

[a] Values are the mean ± SEM expressed in milli-Newtons per square centimeter; $n = 4$.

* $p < 0.01$ vs the individual vehicle.

Table II

Real-time PCR analysis of IL-13 and IL-4 mRNA expression of small intestine from mice treated/infected with vehicle, IL-13, or *N. brasiliensis*[a]

Mice	Treated/infected	IL-13	IL-4
Wild type	Vehicle	1.0 ± 0.2	1.0 ± 0.3
	N. brasiliensis infected	1438 ± 216*	119 ± 30*
	IL-13 treated	ND	1.9 ± 0.7
Stat6$^{-/-}$	Vehicle	1.0 ± 0.2	1.0 ± 0.5
	N. brasiliensis infected	1313 ± 207*	173 ± 52*
	IL-13 treated	ND	1.5 ± 0.6
IL-13$^{-/-}$	Vehicle	ND	1.0 ± 0.3
	N. brasiliensis infected	ND	173 ± 32*
IL-4$^{-/-}$	Vehicle	1.0 ± 0.8	ND
	N. brasiliensis infected	341 ± 73*†	ND

[a] Values are the means ± SEM representing the fold-changes in mRNA expression relative to the individual vehicles; $n = 4$.

* $p < 0.01$ vs vehicle.

† $p < 0.01$ vs WT *N. brasiliensis* infected.